Arabian Journal of Chemistry (2016) 9, 835–845

King Saud University

Arabian Journal of Chemistry

www.ksu.edu.sa
www.sciencedirect.com

ORIGINAL ARTICLE

Green synthesis of Pd@graphene nanocomposite: Catalyst for the selective oxidation of alcohols

Abdulhadi H. Al-Marri [a], Merajuddin Khan [a], Mohammed Rafi Shaik [a], Nils Mohri [b], Syed Farooq Adil [a], Mufsir Kuniyil [a], Hamad Z. Alkhathlan [a], Abdulrahman Al-Warthan [a], Wolfgang Tremel [b], Muhammad Nawaz Tahir [b], Mujeeb Khan [a,*], Mohammed Rafiq H. Siddiqui [a,*]

[a] *Department of Chemistry, College of Science, King Saud University, P.O. Box 2455, Riyadh 11451, Saudi Arabia*
[b] *Institute of Inorganic and Analytical Chemistry, Johannes Gutenberg-University of Mainz, Germany*

Received 18 November 2015; accepted 14 December 2015
Available online 21 December 2015

KEYWORDS

Graphene;
Palladium NPs;
Natural products;
Green chemistry;
Catalysis;
Aromatic alcohols oxidation

Abstract Due to their excellent physicochemical properties and synergistic effect, graphene metallic NPs based nanocomposites have gained significant attention in various technological fields including catalysis. Here we demonstrate a single pot, facile and environmental friendly synthesis of catalytically active palladium(Pd)@graphene nanocomposites (SP-HRG-Pd) by the simultaneous reduction of graphene oxide (GRO) and $PdCl_2$ using *Salvadora persica* L. (miswak) root extract (RE) as bioreductant. The synthesis of SP-HRG-Pd was confirmed by various spectroscopic and microscopic techniques, including ultraviolet–visible (UV–vis), Fourier-transform infrared (FT-IR), Raman and X-ray photoelectron (XPS) spectroscopy, X-ray powder diffraction (XRD) and transmission electron microscopy (TEM). The polyphenolic (flavonoids) and terpenoids rich contents of the miswak RE not only facilitated the reduction of graphene oxide and $PdCl_2$ but also ensured the homogeneous binding of the Pd NPs on graphene, and through stabilization of the surface of SP-HRG-Pd nanocomposites. This also led to the enhanced dispersibility of as synthesized nanocomposites in aqueous solutions. The as-prepared SP-HRG-Pd nanocomposites also demonstrated excellent catalytic activity toward the selective oxidation of aromatic alcohols. Furthermore, in order to study the effect of calcination temperature and concentration of Pd NPs on the catalytic activities of nanocomposites, different samples of SP-HRG-Pd nanocomposites containing different amounts of Pd using various concentrations of Pd precursor were prepared and calcined at various temperatures.

* Corresponding authors.
E-mail addresses: kmujeeb@ksu.edu.sa (M. Khan), rafiqs@ksu.edu.sa (M.R.H. Siddiqui).
Peer review under responsibility of King Saud University.

Production and hosting by Elsevier

http://dx.doi.org/10.1016/j.arabjc.2015.12.007

1. Introduction

Graphene/inorganic nanoparticles based nanocomposites have attracted tremendous attention as a new class of hybrid materials (Mahmood et al., 2014; Bonaccorso et al., 2015). The interest of scientific community in these materials has been ever-growing, due to their peculiarities in combining desirable properties of building blocks for a given application (Li et al., 2015). The novel catalytic, magnetic and optoelectronic properties of graphene nanocomposites based on the hybridization with nanoparticles (NPs) have been exploited in various applications, including catalysis, electronics, imaging, and energy storage (Navalon et al., 2014; Xia et al.,2014; Luo and Zhi, 2015; Vashist and Luong, 2015). So far, great efforts have been made to uniformly combine different varieties of nanomaterials, including metal and metal oxide NPs with graphene, which significantly enhanced the properties of these materials due to synergistic effect as result of their combination (Wang et al., 2014; Ullah et al., 2015). Apart from enhancing the properties of graphene, the NPs also act as stabilizers against the aggregation of individual graphene sheets, which is greatly caused by the strong Van der Waals interactions between graphene layers (Tang et al., 2014). Furthermore, in many cases the intercalation of metallic NPs with graphene also facilitated the exfoliation of individual graphene layers from graphite (Gotoh et al., 2011). Therefore, more efforts and new strategies to synthesize graphene based nanocomposites are indispensable (Zhang et al., 2014b).

The binding of metallic NPs on graphene for the preparation of graphene based nanocomposites is generally categorized by two different methods (Zhu et al., 2010), (i) the *post immobilization* (*ex situ* hybridization) and (ii) *in situ* binding (*is situ* crystallization). The *post immobilization* involves the mixing of separate solutions of graphene nanosheets and pre-synthesized or commercially available NPs (Xia et al., 2014). On the other hand, *in situ* binding of NPs is carried out via simultaneous reduction of respective metallic salts and graphene oxide (GRO) with various reductants (Bhirud et al., 2015). Commonly, the methods involving *in situ* binding of NPs have been widely used due to their cost effectiveness as they reduce the number of steps to get desire product (Leng et al., 2014). Several reduction techniques have been applied during *in situ* preparation of graphene nanocomposites, e.g. chemical, thermal and electrochemical. Among them chemical reduction is the most promising and widely applied method for the large scale production of graphene metallic NPs based nanocomposites (Stankovich et al., 2006; Bai and Shen, 2012; Khan et al., 2013b, 2014c, 2015b).

Various nanocomposites have been prepared via *in situ* chemical reduction of different metal precursors, such as $HAuCl_4$, $AgNO_3$, K_2PtCl_4, H_2PdCl_6 by reductants such as hydrazine hydrate, amines, and $NaBH_4$ (Compton and Nguyen, 2010; Xu et al., 2008; Zhang et al., 2014a; Han et al., 2013). However, nanocomposites prepared from chemical methods usually suffer from irreversible aggregations and poor dispersibility of NPs on the surface of graphene, which require surface functionalization of the NPs *and/or* graphene sheets to enhance processability of these materials (Kuila et al., 2012; Dey et al., 2015). Furthermore, majority of the chemicals involved during the *in situ* reduction and functionalization of nanocomposites are highly toxic in nature, which are harmful to both environment and human life (Kuila et al., 2013). In addition, the presence of trace amount of these highly toxic reducing agents on the surface of the nanocomposites could seriously alter the properties of these materials and have adverse effects on their biological applications (Yin et al., 2015).

Recently, the trends of applying green reductants in the synthesis of nanomaterials have gained popularity (Adil et al., 2015b). For instance, a variety of green reductants have been applied for the synthesis of metallic NPs, such as plant extracts, vitamin C, amino acids, ascorbic acid, glucose, bovine serum albumin and microorganisms (Hebbalalu et al., 2013; Nadagouda and Varma, 2007; Bahram et al., 2014; Khan et al., 2013a; Hulkoti and Taranath, 2014). Among these green reductants, plant extracts have received significant attention due to their cost effectiveness, easy availability and bulk amounts (Akhtar et al., 2013; Barman et al., 2013). Furthermore, plant extracts not only act as reducing agents but also function as stabilizing agents, which limit the use of additional chemical stabilizers (Khan et al., 2014b; Makarov et al., 2014). Due to this, plant extracts have not only been used for the synthesis of metallic NPs, but in many cases, they have also been successfully applied for the reduction of graphene oxide (GRO) (Khan et al., 2014b). Although a series of metallic NPs have been prepared using plant extracts as reducing agents, their application in the synthesis of graphene based nanocomposites has so far been limited (Sedki et al., 2015).

In our previous study, we have successfully demonstrated a simple, one-step approach for the preparation of graphene/Ag nanocomposites via simultaneous reduction of both graphene oxide (GRO) and silver ions using *Pulicaria glutinosa* plant extract (PE) as reducing agent (Al-Marri et al., 2015). In this study, we demonstrate the synthesis of catalytically active Pd@graphene (HRG-Pd) nanocomposites using *Salvadora persica* (SP) L. (miswak) extract as a bioreductant (cf. Scheme 1). *S. persica* L. is commonly known as miswak, which literally means 'tooth-cleaning stick or chewing stick' and has been widely used as oral hygiene tool (Almas and Almas, 2014). It is a glabrous tree or shrub belonging to the family *Salvadoraceae* and found in many parts of the world (Halawany, 2012; Fatemeh et al., 2012). The root extract of miswak is rich in various classes of phytomolecules including terpenoids, alkaloids, flavonoids, saponins and tannins, which have been known to possess remarkable reduction properties (Akhtar et al., 2011; Alam et al., 2013). Indeed, the excellent reducing ability of the root extract of miswak has been exploited for the first time in our previous study for the reduction of GRO (Khan et al., 2015a).

Herein, the *S. persica* L (*S. persica* L.) root extract (RE) acted as both reducing agent and *in situ* functionalization ligand, which facilitated the binding of Pd NPs onto surface of HRG sheets. The as-prepared SP-HRG-Pd nanocomposites were characterized by ultraviolet–visible absorption (UV–Vis) spectroscopy, X-ray powder diffraction (XRD), Fourier-transform infrared spectroscopy (FT-IR), X-ray photoelectron spectroscopy (XPS), and transmission electron microscopy (TEM). Furthermore, the HRG-Pd nanocomposites that are known to possess excellent catalytic activities toward a variety of organic transformations are tested for the catalytic oxidation of various alcohols (Hsu and Chen, 2014l; Herves et al., 2012; Adil et al., 2015a).

2. Material and method

2.1. Materials used

The roots of *S. persica* L. growing in Jizan, Southern region of Saudi Arabia were purchased from a local herbal market at Batha, Riyadh, Saudi Arabia. A plant taxonomist from the Herbarium Division of the College of Science, King Saud University, Riyadh, Saudi Arabia, confirmed the identity of the plant material. A voucher specimen is retained in our laboratory with the voucher specimen number KSUHZK-302. Graphite powder (99.999%, _200 mesh) was purchased from Alfa Aesar (USA). Palladium (II) Chloride ($PdCl_2$ 99.99%, Sigma Aldrich, USA), Concentrated sulfuric acid (H_2SO_4 98%), potassium permanganate ($KMnO_4$ 99%), sodium nitrate ($NaNO_3$, 99%) and hydrogen peroxide (H_2O_2, 30 wt%) and all organic solvents were obtained from Aldrich Chemicals (USA) and used without further purification.

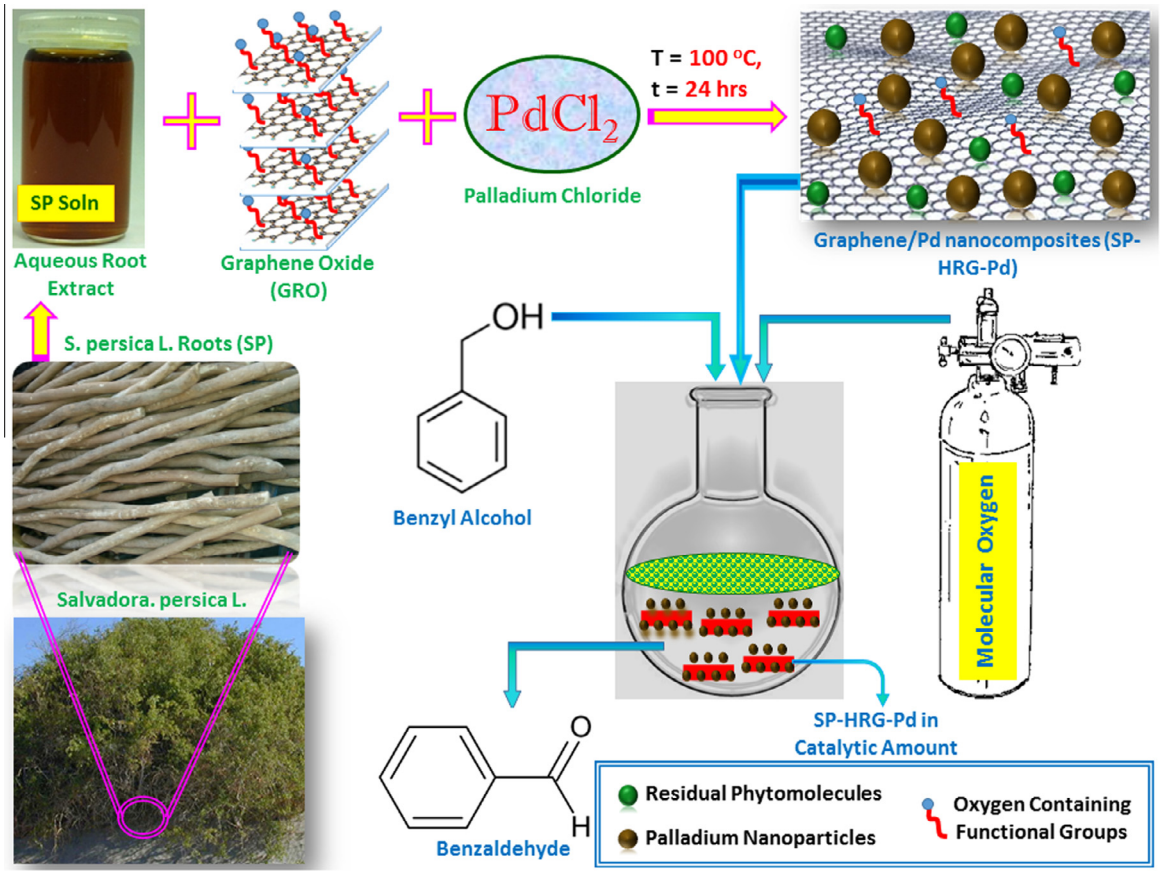

Scheme 1 Schematic illustration of the green synthesis of Pd@graphene (SP-HRG-Pd) nanocomposites using *Salvadora persica* L. root extract (RE) as bioreductant. The as prepared nanocomposite is also applied as oxidation catalyst for the transformation of various alcohols.

2.2. Preparation of S. persica L. root (miswak) extract

First, fresh roots of *S. persica* L. were cut into small pieces (~5 to 35 mesh). These pieces (1.3 kg) were soaked in deionized water (3000 mL) and refluxed for 4 h. The aqueous solution obtained after reflux was filtered and dried at 50 °C under reduced pressure in a rotary evaporator to give a dark brownish gummy extract (30.0 g) which was stored at 0–4 °C for further use.

2.3. Preparation of Pd@graphene nanocomposite (SP-HRG-Pd-1)

Graphite oxide (GO) used for the preparation of SP-HRG-Pd-1 was synthesized according to our previously reported method (Khan et al., 2014a). Initially, as-prepared graphite oxide or GO (200 mg) was dispersed in 40 mL of DI water and sonicated for 30 min to obtain graphene oxide (GRO) sheets. The resulting suspension was taken in a round bottom flask and was added to 100 mg (0.563 mmol) of $PdCl_2$. The flask was mounted with a cooling condenser, which is heated to 100 °C. Subsequently, 10 mL of an aqueous solution of the root extract (0.1 g mL^{-1}) was added to the suspension, which was then allowed to stir for 24 h at 98 °C. Afterward the resulting black powder of (SP-HRG-Pd-1) was collected by filtration, and further washed with DI water several times to remove excess root extract residue and redistributed into water for sonication. This suspension was centrifuged at 4000 rpm for another 30 min. The final product was collected by vacuum filtration and dried in vacuum. The obtained catalyst was calcined at different temperatures such as 300 °C, 400 °C, 500 °C which was subjected to catalytic evaluation for the conversion of benzyl alcohol to benzaldehyde.

2.4. Evaluation of catalytic performance

In a typical reaction, 300 mg of catalyst was loaded in a glass flask pre-charged with 0.2 mL (2 mmol) benzyl alcohol in 10 mL toluene as solvent; the mixture was then heated to 100 °C with vigorous stirring. Oxygen was bubbled at a flow rate of 20 mL min^{-1} into the mixture once the reaction temperature was attained. After reaction, the solid catalyst was separated by centrifugation and the liquid samples were analyzed by gas chromatography to evaluate the conversion of the desired product by (GC, 7890A) Agilent Technologies Inc, equipped with a flame ionization detector (FID) and a 19019S-001 HP-PONA column.

2.5. Characterization

A Perkin Elmer lambda 35 (USA) UV–vis spectrophotometer was used for the optical measurements. The analysis was

performed in quartz cuvettes using DI water as a reference solvent. Stock solutions of SP-HRG-Pd-1 and GRO for the UV measurements were prepared by dispersing 5 mg of sample in 10 mL of DI water and sonicating for 30 min. The UV samples of GRO and SP-HRG-Pd-1 were prepared by diluting 1 mL of stock solution with 9 mL of water.

XRD diffractograms were collected on a Altima IV [Rigaku, Japan] X-ray powder diffractometer using Cu Kα radiation (λ = 1.5418°A).

Transmission electron microscopy (TEM) was performed on a JEOL JEM 1101 (USA) transmission electron microscope. The samples for TEM were prepared by placing a drop of primary sample on a holey carbon copper grid and drying for 6 h at 80 °C in an oven.

Fourier transform infrared spectrometer (FT-IR) spectra were measured on a Perkin–Elmer 1000 (USA) Fourier transform infrared spectrometer. In order to remove any free biomass residue or unbound extract to the surfaces of SP-HRG-Pd-1 sheets, the SP-HRG-Pd nanosheets were washed repeatedly with distilled water, and then the product was centrifuged at 9000 rpm for 30 min and dried. The purified SP-HRG-Pd nanosheets were mixed with KBr powder and pressed into a pellet for measurement. Background correction was made using a reference blank KBr pellet.

X-ray photoelectron spectroscopy (XPS) spectra were measured on a PHI 5600 Multi-Technique XPS (Physical Electronics, Lake Drive East, Chanhassen, MN) using monochromatized Al Kα at 1486.6 eV. Peak fitting was performed using the CASA XPS Version 2.3.14 software.

3. Results and discussion

The excellent reducing ability of *S. persica L.* root extract is exploited for the environmental friendly synthesis of catalytically active Pd@graphene (SP-HRG-Pd) nanocomposites. The synthesis of nanocomposite is carried out in a single step via simultaneous reduction of GRO and $PdCl_2$ under facile conditions using *S. persica L.* RE as both reducing as well as stabilizing agent. During the synthesis, the root extract added to the aqueous dispersion of GRO and $PdCl_2$ is allowed to stir under reflux conditions for several hours. The gradual color change from dark brown to black observed during the process indicated the formation of Pd@graphene (SP-HRG-Pd) nanocomposites.

Usually, graphene based nanocomposites synthesized by chemical methods suffer from poor dispersibility due to the removal of oxygen containing functional groups during the reduction process. However, the phytomolecule contents of the root extract, including flavonoids and terpenoids facilitates the stabilization of the surfaces of SP-HRG-Pd nanocomposite and enhanced its dispersibility. Furthermore, these phytomolecules not only help to enhance the dispersibility of the nanocomposites but also contribute to the homogeneous distribution of the Pd NPs on the surface of the graphene nanosheets. This has a significant effect on the catalytic activity of the as-prepared nanocomposite. Additionally, to study the effect of the concentration of Pd NPs on the catalytic activities of SP-HRG-Pd nanocomposites, different samples are prepared by varying the concentration of Pd NPs on the surface of HRG. For instance, SP-HRG-Pd-1 and 2 are prepared by taking 50 and 75 wt% of $PdCl_2$ with those of GRO, whereas the amount of RE was kept constant during this process.

3.1. UV–Vis spectroscopy

The initial monitoring of the formation of SP-HRG-Pd was carried out by measuring the UV–Vis spectra of GRO, root extract, $PdCl_2$ and SP-HRG-Pd-1 as shown in Fig. 1. The GRO has typically two absorption bands at ~230 and ~301 nm, whereas $PdCl_2$, has a characteristic absorption band at ~420 nm. The disappearance of these bands in the UV spectrum of SP-HRG-Pd-1 and an emergence of new band at ~280 nm, which is the characteristic band of highly reduced graphene oxide (HRG) (Khan et al., 2014a), clearly point toward the simultaneous reduction of both GRO and $PdCl_2$ and also indicate the formation of nanocomposite. Additionally, the root extract mediated reduction product (SP-HRG-Pd-1) exhibited an extra absorption band at ~323 nm (Fig. 1 red line), which is due to the RE phytomolecules bound to the SP-HRG-Pd nanocomposites surfaces as confirmed by comparing the absorption spectra of SP-HRG-Pd-1 and pure RE.

3.2. X-ray diffraction (XRD)

The formation of SP-HRG-Pd -1 and the crystallinity of the nanocomposite were further confirmed by XRD analysis. For this purpose, XRD patterns of pure graphite, graphene oxide and SP-HRG-Pd-1 were measured (cf. Fig. 2). Pristine graphite showed a characteristic intense reflection at 26.4°, which is shifted to the lower brag angle in GRO at 10.9° during the course of oxidation of graphite. However, the disappearance of the reflection at 10.9° corresponding to the GRO and the appearance of a broad reflection centered at ~22.4° in SP-HRG-Pd-1 confirm the reduction of GRO and also point toward the formation of few layer graphene (45). Moreover, the XRD pattern of SP-HRG-Pd-1 also exhibited distinct reflections at 40.02° (1 1 1), 46.49° (2 0 0), 68.05° (2 2 0), 81.74° (3 1 1) and 86.24° (2 2 2), apart from other weak reflections. The presence of these reflections confirms the formation of Pd nanoparticles. Further indexing of these reflections reveals the face centered cubic (*fcc*) structure of Pd NPs on the surface of HRG (JCPDS: 87-0641, space group: Fm3m (2 2 5)).

3.3. Fourier transforms infrared spectrometer (FT-IR)

The simultaneous reduction of GRO and $PdCl_2$, their synthesis and surface stabilization of SP-HRG-Pd nanocomposites are also confirmed by FT-IR analysis. Fig. 3 shows the FT-IR spectra of GRO, SP-HRG-Pd-1 and pure *S. persica* L. RE. Commonly the reduction of GRO is confirmed by the reduced intensities of the IR peaks in the FT-IR spectra of graphene, which is caused by the removal of the oxygen containing functional groups. In the case of SP-HRG-Pd-1, the bands at ~1740 cm^{-1} (for C═O stretching) and ~1630 cm^{-1} (for C═C stretching) belonging to the GRO disappeared. In addition, there was relative decrease in the intensities of some of the prominent bands of GRO, such as a broad band at around 3440 cm^{-1} for hydroxyl groups, confirmed the reduction of GRO. Furthermore, in order to confirm the presence of the phytomolecules of the root extract (RE) on the surface of

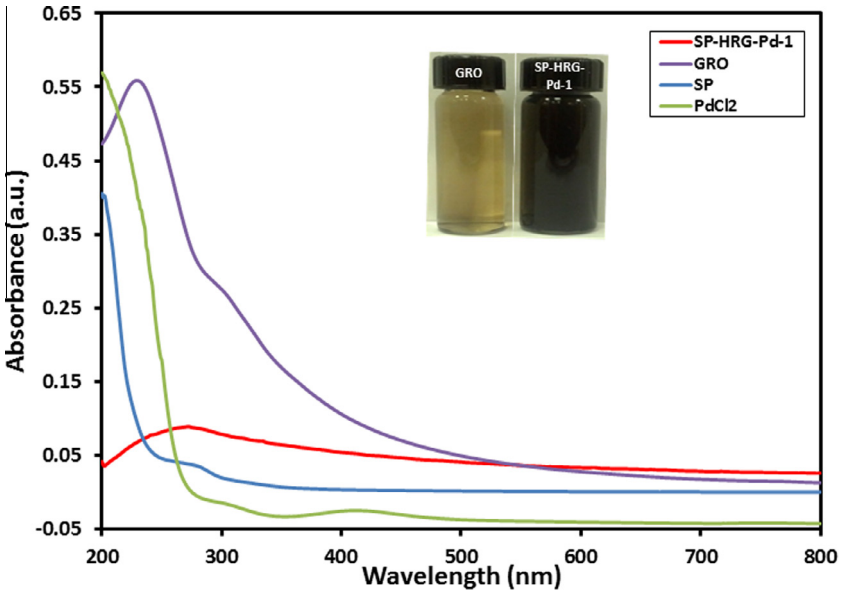

Figure 1 UV–Vis absorbance spectra of Pd@graphene nanocomposite 50 wt% (SP-HRG-Pd-1), graphene oxide (GRO), pure *S. persica* L. RE (SP) and $PdCl_2$ salt.

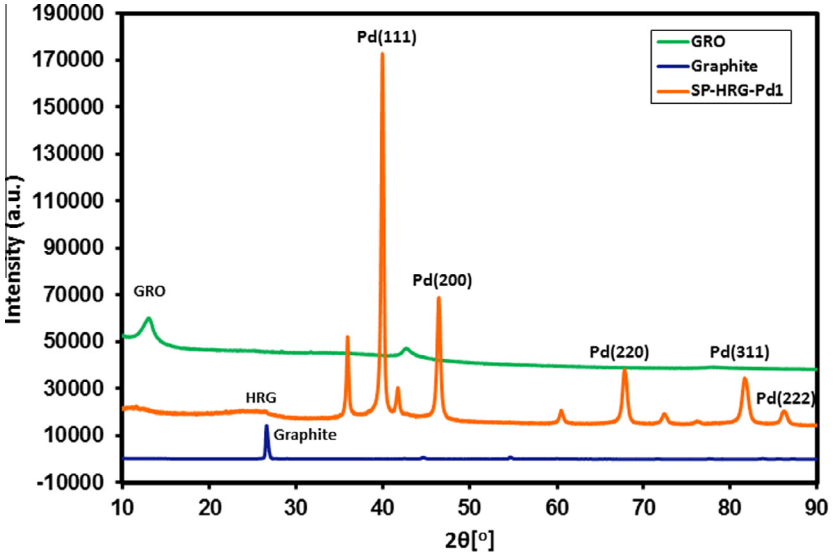

Figure 2 XRD patterns of graphite (blue), graphene oxide (GRO) (green), RE mediated Pd@graphene nanocomposite 50 wt% (SP-HRG-Pd-1) (orange).

SP-HRG-Pd-1 as stabilizers, its IR spectrum is compared with that of the pure RE. This revealed that, a majority of the IR peaks belonging to the root extracts also present in the FT-IR spectrum of the SP-HRG-Pd-1. These peaks are either present at the same positions or slightly shifted. For instance, the presence of the bands at ~2921 cm^{-1}, ~2849 cm^{-1}, 1698 cm^{-1} and 1122 cm^{-1} in SP-HRG-Pd-1, which also appear in IR spectrum of root extract but are absent in GRO strongly suggests that the phytomolecules of miswak root extract act not only as bioreductant, but also act as stabilizers on the surface of the SP-HRG-Pd-1 sheets.

3.4. X-ray photoelectron spectroscopy (XPS)

Surface composition of SP-HRG-Pd was investigated via X-ray photoelectron spectroscopy (XPS). Fig. 4 shows a low-resolution spectrum over the whole binding energy (a) and a high-resolution spectrum of the carbon (b) and Pd (c) signal. The surface is composed of mainly carbon and oxygen, as expected for the RE. The Pd 3d signal at 336 eV confirms the existence of Pd on the RE. Remaining signals of low intensity can be attributed to nitrogen, usually found adsorbed on the sample surface and chloride from unreacted $PdCl_2$.

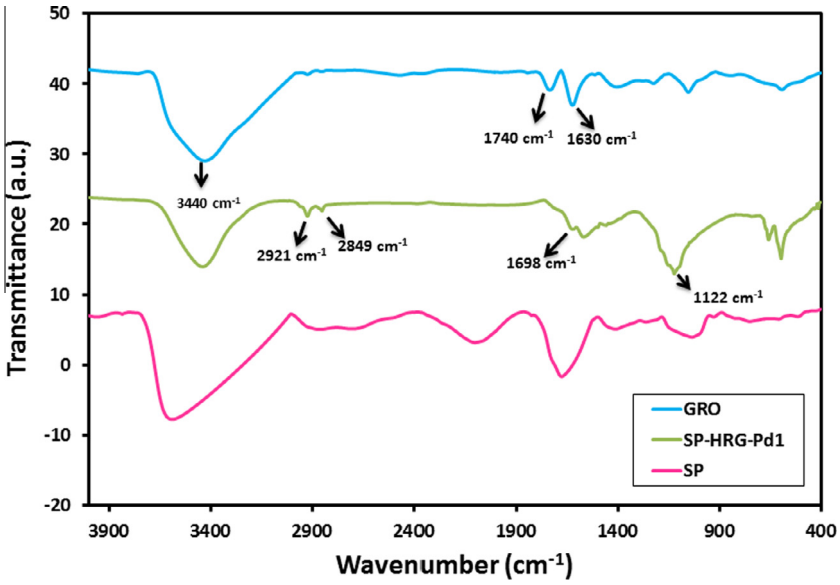

Figure 3 FT-IR spectra of graphene oxide (GRO), RE-mediated Pd@graphene nanocomposite 50 wt% (SP-HRG-Pd1) and pure *S. persica* L. RE.

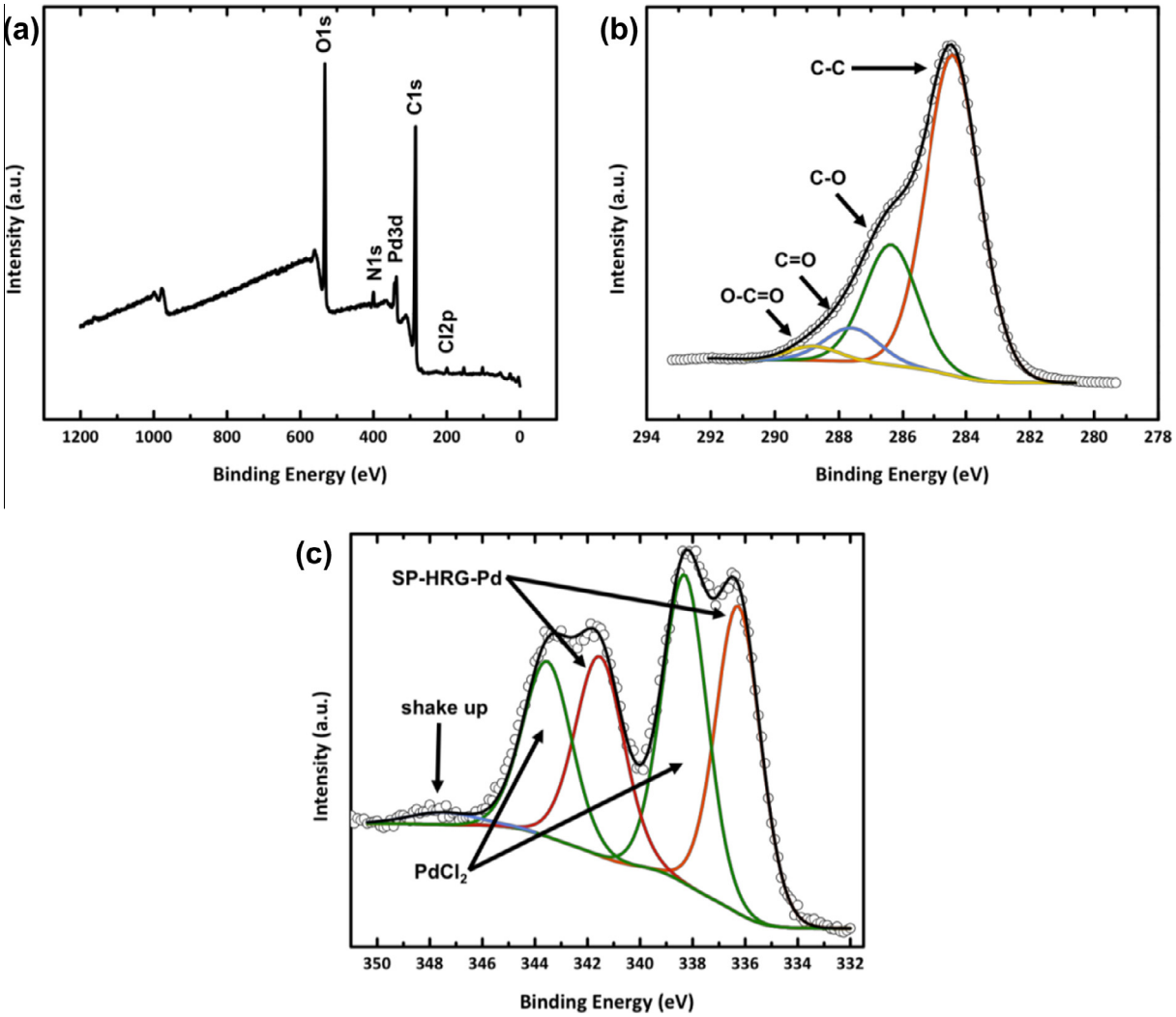

Figure 4 XPS spectra of Pd@graphene nanocomposite. Low-resolution spectrum over whole binding energy range (a), high-resolution spectrum of carbon signal (b) and Pd signal (c).

High-resolution analysis of the carbon signal reveals it to consist of four distinct peaks at 284.4, 286.4, 287.6 and 288.8 eV, which can be attributed to C—C, C—O, C═O and O—C═O groups respectively. The low intensity of the C—O signal confirms the successful reduction to HRG (Khan et al., 2014a). The Pd signal consists of two doublets, originating from SP-HRG-Pd and unreacted $PdCl_2$. Intensity of both signals is about the same, showing that 50% of applied $PdCl_2$ reacted to form SP-HRG-Pd.

3.5. Raman spectra

Furthermore, the presence of highly reduced graphene in the SP-HRG-Pd composite is also confirmed by the Raman analysis. For this purpose, the Raman spectrum of SP-HRG-Pd-1 is compared with that of GRO, as shown in Fig. 5. Generally, graphene exhibits two main peaks in the Raman spectrum, the G and D bands at 1575 and 1350 cm^{-1}, respectively. However, in GRO, the G and the D bands are shifted and appear at 1602 and 1340 cm^{-1}, respectively, due to the destruction of the sp^2 character by the extensive oxidation (Gurunathan et al., 2013). After the reduction with *S. Persica* L. root extract these bands are relocated toward their ideal positions. For instance, the G band in SP-HRG-Pd is shifted by ~10 cm^{-1} from 1602 to 1592 cm^{-1}, whereas a slight shift was observed in the D band from 1340 to 1336 cm^{-1}. These changes in the Raman spectrum of SP-HRG-Pd after the reduction clearly points toward the reduction of GRO in the composite.

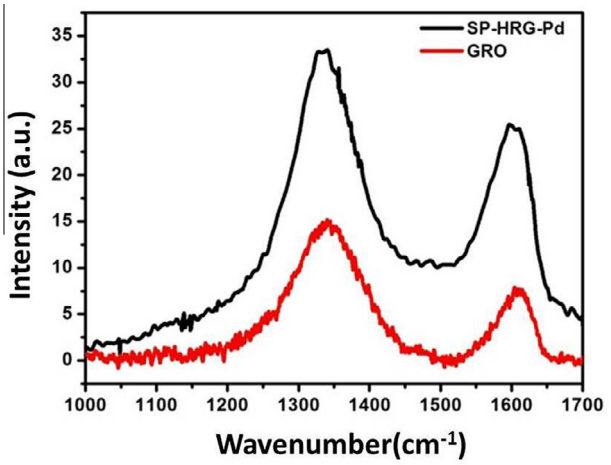

Figure 5 Raman spectra of graphene oxide (GRO) and Pd@graphene nanocomposites (SP-HRG-Pd).

3.6. Transmission electron microscopy (TEM)

The morphology and the structure of Pd NPs on the surface of HRG in the SP-HRG-Pd composite are analyzed via transmission electron microscopy (TEM). The overview image in Fig. 6a shows the presence of small and spherical shape Pd NPs on the surface of HRG, whereas the magnified images in Fig. 6b and c further confirm the shape and crystallinity of these NPs. The Pd NPs are not adsorbed chemically, but are held via physisorption on the surface of graphene by Van der Waals interactions. Furthermore, the elemental composition of the as-synthesized SP-HRG-Pd composite was also determined via EDX, as shown in Fig. 7. The presence of both HRG and Pd NPs is clearly indicated in the spectrum, together with other elements including carbon and oxygen. This also indicates the presence of residual phytomolecules of the plant extract as capping ligands on the surfaces of the NPs.

3.7. Catalytic application of SP-HRG-Pd nanocomposites

In order to comprehend the amount of Pd NPs on graphene, which can be suitable for catalytic performance, catalysts are synthesized with varying amount of Pd NPs supported on graphene, which were 50 wt% (SP-HRG-Pd-1) and 75 wt% (SP-HRG-Pd-2) of graphene. Calcination temperatures play an important role in the catalytic performance of the synthesized material, which is confirmed in our previous study (Alabbad et al., 2014). Therefore, the as synthesized catalysts are calcined at different temperatures such as 300 °C, 400 °C and 500 °C before being subjected to the catalytic evaluation studies. When the catalyst SP-HRG-Pd-1 (50 wt%) calcined at 300 °C employed for the conversion of benzyl alcohol to benzaldehyde, only 24.08% conversion is observed after one hour, and a maximum of 96.64% conversion is obtained upon continuation of the reaction for almost three hours.

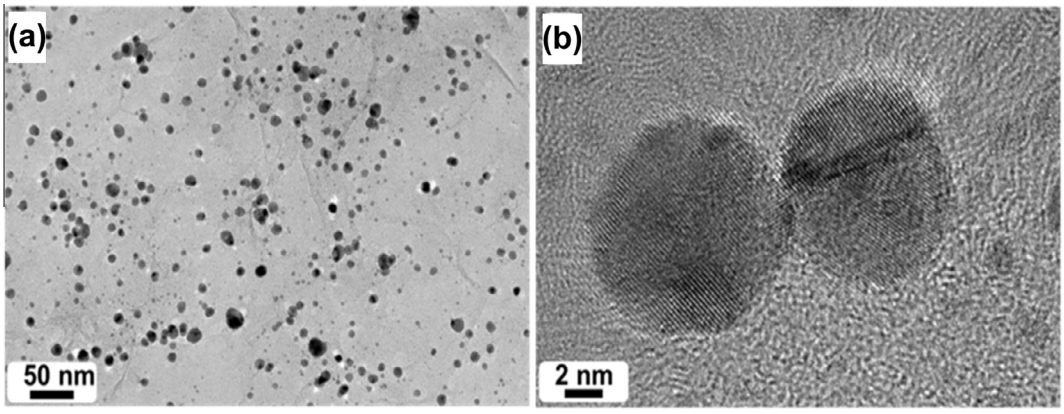

Figure 6 Transmission electron microscopic (TEM) images of the SP-HRG-Pd composite (a) overview and (b) magnified HRTEM images, which confirm the crystallinity of the composite.

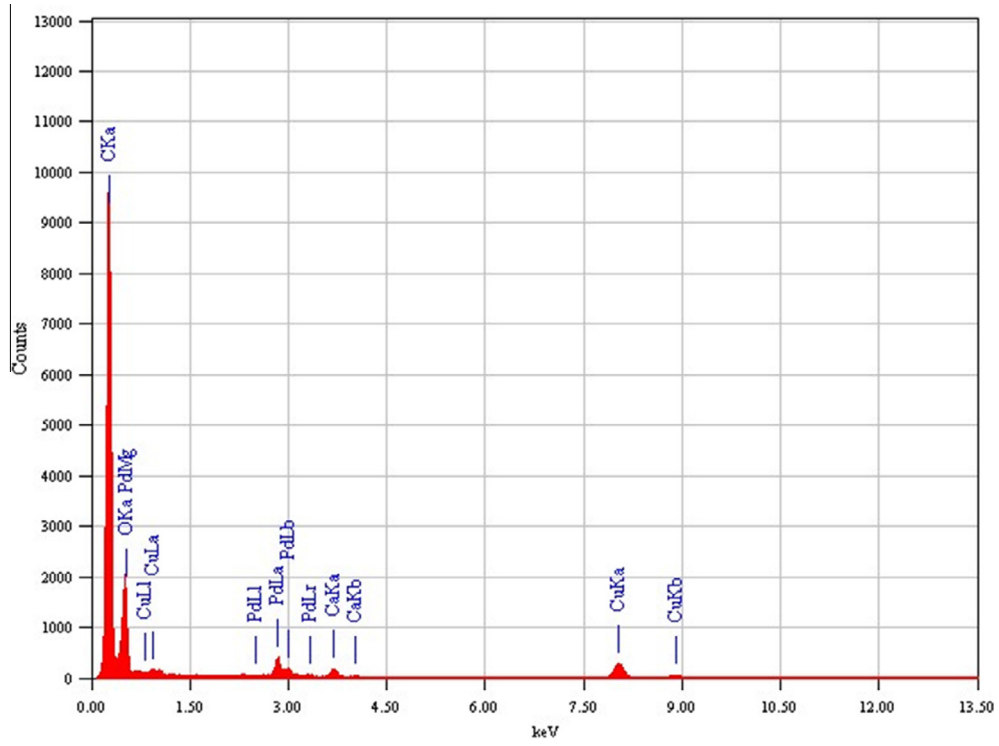

Figure 7 Energy dispersive X-ray spectrum (EDX) of as-synthesized SP-HRG-Pd composite confirming the presence of Pd NPs together with HRG.

However, when the same catalyst is calcined at temperatures 400 °C and 500 °C, a 100% conversion of product is obtained. Furthermore, it is observed that the catalyst calcined at 400 °C, gave after 3 mins of reaction time a 35% conversion while a 100% conversion was observed after 15 min. The 500 °C calcined catalyst yielded similar conversion in 45 min. Hence, it can be concluded that the catalyst calcined at 400 °C displays best catalytic performance. The catalyst SP-HRG-Pd-2 is also subjected to similar studies, where it is calcined at different temperatures such as 300 °C, 400 °C and 500 °C and then tested for the conversion of benzyl alcohol to benzaldehyde (cf. Fig. 8). It is found that the all catalysts, i.e. calcined at different temperatures, yielded 100% conversion, however the time taken for such conversion is different. For instance, the reaction is completed in 135 min, 30 min and 60 min for the catalyst calcined at 300 °C, 400 °C and 500 °C, respectively. Hence, from the comparison of the results obtained by using both the catalyst compositions, it is confirmed that the catalyst calcined at 400 °C displayed best catalytic performance with both catalysts. Since the graphene support is employed in order to reduce the metal loading in the catalyst, SP-HRG-Pd-1, the catalyst with less percentage of Pd (i.e. 50% w/w of graphene), calcined at 400 °C, is selected for further studies. A graphical illustration of the results obtained is given in Fig. 8.

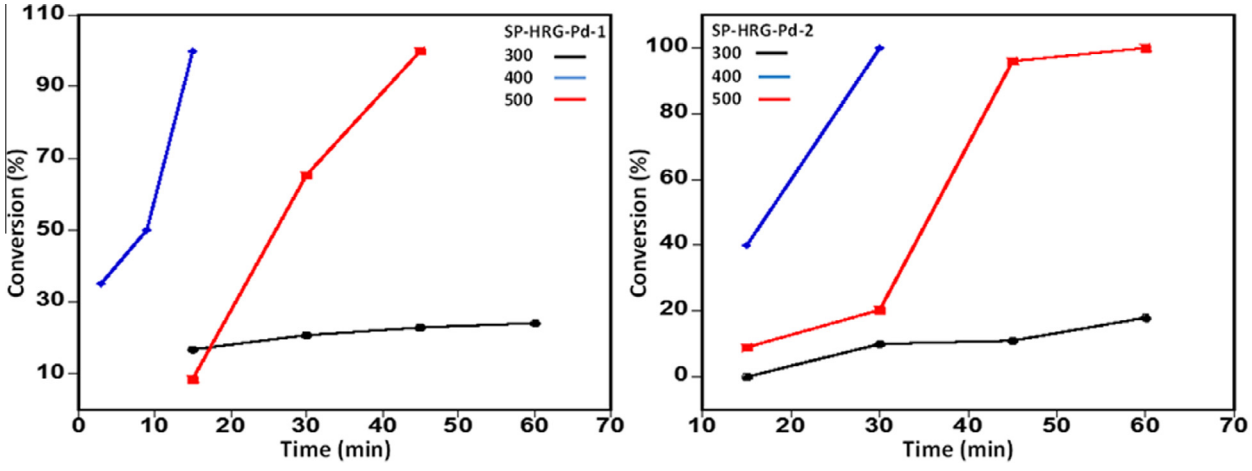

Figure 8 Graphical illustration of conversion vs time for the catalyst SP-HRG-Pd-1 and SP-HRG-Pd-2 calcined at different temperatures.

To further investigate the catalytic performance of the above mentioned catalyst toward various substrates, the catalyst SP-HRG-Pd-1 calcined at 400 °C was employed for oxidation of a series of substituted benzyl alcohols, containing 4—CH_3, 4—OCH_3, 4—Cl, 4—NO_2, 4—$C(CH_3)_3$, 4—CF_3 and 3—NO_2 groups. All reactions were carried out under similar set of conditions for the conversion to corresponding aldehyde product. It is observed that conversion product obtained varied from 2% to 100% and the time from 15 to 60 min. In order to study the activity of the same catalyst toward aliphatic alcohols, citronellol, an aliphatic alcohol, is subjected to oxidation reaction using the catalyst SP-HRG-Pd-1 calcined at 400 °C under similar reaction conditions. No oxidation product is observed, which indicates that the catalyst is highly selective toward the oxidation of aromatic alcohols. These results are summarized in Table 1.

Table 1 Selective oxidation of benzyl alcohol and its derivatives into corresponding aldehydes in the presence of O_2 as clean oxidant.

R. no.	Reactants	Products	Time taken (min)	Conversion (%)	Selectivity (%)
1	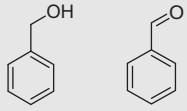		15	100	> 99
2	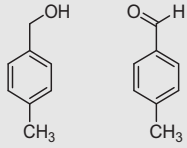		15	100	> 99
3	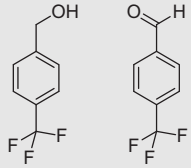		30	100	> 99
4	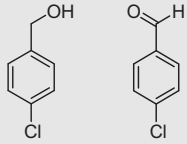		60	50.2	> 99
5	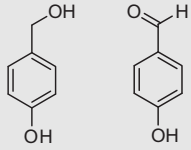		60	43.5	> 99
6	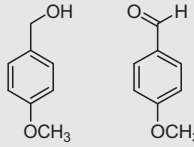		60	30	> 99
7	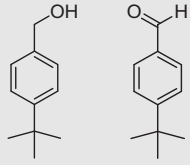		60	20.3	> 99
8	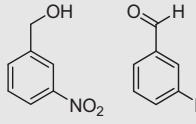		60	2.03	> 99

4. Conclusion

In this study, we have successfully demonstrated a green approach for the synthesis of catalytically active Pd@graphene nanocomposites (SP-HRG-Pd) using *S. persica* L. RE (miswak) as a bioreductant. Using this method, crystalline and spherical-shaped Pd NPs, homogeneously distributed on the surface of graphene without using any harmful reducing or capping agents are formed. Due to the enhanced dispersibility of the SP-HRG-Pd nanocomposites by the stabilization of the phytomolecules of the RE, the as-prepared nanocomposites have demonstrated excellent catalytic activities toward the oxidation of various aromatic alcohols. The detailed catalytic studies of SP-HRG-Pd nanocomposites at different calcination temperatures revealed that both nanocomposites exhibited oxidation property. However, the SP-HRG-Pd-1, the catalyst with less percentage of Pd (i.e. 50% w/w of graphene), calcined at 400 °C, is explored for further studies and exhibited excellent catalytic activity for the oxidation of various alcohols, displaying selectivity toward aromatic alcohols. Therefore, the eco-friendly approach for the synthesis of graphene metallic NPs based nanocomposites can be easily exploited for the large-scale synthesis of graphene-based nanocatalysts that have potential applications in various organic transformations including oxidation.

Acknowledgements

This project was funded by National Plan for Science, Technology and Innovation (MAARIFAH), King Abdulaziz City for Science and Technology, Kingdom of Saudi Arabia, Award Number (11NAN-1860-02).

References

Adil, S.F., Alabbad, S., Kuniyil, M., Khan, M., Alwarthan, A., Mohri, N., Tremel, W., Tahir, M.N., Siddiqui, M.R.H., 2015a. Vanadia supported on nickel manganese oxide nanocatalysts for the catalytic oxidation of aromatic alcohols. Nanoscale Res. Lett. 10, 52.

Adil, S.F., Assal, M., Khan, M., Al-Warthan, A., Siddiqui, M.R.H., Liz-Marzán, L.M., 2015b. Biogenic synthesis of metallic nanoparticles and prospects toward green chemistry. Dalton Trans. 44, 9709–9717.

Akhtar, J., Siddique, K.M., Bi, S., Mujeeb, M., 2011. A review on phytochemical and pharmacological investigations of miswak (*Salvadora persica* Linn). J. Pharm. Bioall. Sci. 3, 113–117.

Akhtar, M.S., Panwar, J., Yun, Y.-S., 2013. Biogenic synthesis of metallic nanoparticles by plant extracts. ACS Sustain. Chem. Eng. 1, 591–602.

Alabbad, S., Adil, S., Assal, M., Khan, M., Alwarthan, A., Siddiqui, M.R.H., 2014. Gold & silver nanoparticles supported on manganese oxide: synthesis, characterization and catalytic studies for selective oxidation of benzyl alcohol. Arab. J. Chem. 7, 1192–1198.

Alam, M.N., Roy, N., Mandal, D., Begum, N.A., 2013. Green chemistry for nanochemistry: exploring medicinal plants for the biogenic synthesis of metal NPs with fine-tuned properties. RSC Adv. 3, 11935–11956.

Al-Marri, A.H., Khan, M., Khan, M., Adil, S.F., Al-Warthan, A., Alkhathlan, H.Z., Tremel, W., Labis, J.P., Siddiqui, M.R.H., Tahir, M.N., 2015. *Pulicaria glutinosa* extract: a toolbox to synthesize highly reduced graphene oxide–silver nanocomposites. Int. J. Mol. Sci. 16, 1131–1142.

Almas, A., Almas, K., 2014. Miswak (*Salvadora persica* chewing stick): the natural toothbrush revisited. Odontostomatol. Trop. 37, 27–39.

Bahram, M., Hoseinzadeh, F., Farhadi, K., Saadat, M., Najafi-Moghaddam, P., Afkhami, A., 2014. Synthesis of gold nanoparticles using pH-sensitive hydrogel and its application for colorimetric determination of acetaminophen, ascorbic acid and folic acid. Colloids Surf. A: Physicochem. Eng. Aspects. 441, 517–524.

Bai, S., Shen, X., 2012. Graphene–inorganic nanocomposites. RSC Adv. 2, 64–98.

Barman, G., Maiti, S., Laha, J.K., 2013. Bio-fabrication of gold nanoparticles using aqueous extract of red tomato and its use as a colorimetric sensor. Nanoscale Res. Lett. 8, 1–9.

Bhirud, A.P., Sathaye, S.D., Waichal, R.P., Ambekar, J.D., Park, C.-J., Kale, B.B., 2015. In-situ preparation of N-TiO_2/graphene nanocomposite and its enhanced photocatalytic hydrogen production by H_2S splitting under solar light. Nanoscale 7, 5023–5034.

Bonaccorso, F., Colombo, L., Yu, G., Stoller, M., Tozzini, V., Ferrari, A.C., Ruoff, R.S., Pellegrini, V., 2015. Graphene, related two-dimensional crystals, and hybrid systems for energy conve1rsion and storage. Science 347 (6217), 1246501–1246509.

Compton, O.C., Nguyen, S.T., 2010. Graphene oxide, highly reduced graphene oxide, and graphene: versatile building blocks for carbon-based materials. Small 6, 711–723.

Dey, A., Panja, S., Sikder, A.K., Chattopadhyay, S., 2015. One pot green synthesis of graphene–iron oxide nanocomposite (GINC): an efficient material for enhancement of thermoelectric performance. RSC Adv. 5, 10358–10364.

Fatemeh, E.-A., Mahmoud, N.S., Hasan, F., Farah, B.K., Mahin, A., Zahra, H., Hossein, D., Mohammad, A.J., Hossein, B., Faezeh, N., 2012. Study of the effects of natural toothbrush (*Salva-dora persica*) in prevention of dental caries and plaque index. Health 4, 612–618.

Gotoh, K., Kinumoto, T., Fujii, E., Yamamoto, A., Hashimoto, H., Ohkubo, T., Itadani, A., Kuroda, Y., Ishida, H., 2011. Exfoliated graphene sheets decorated with metal/metal oxide nanoparticles: simple preparation from cation exchanged graphite oxide. Carbon 49, 1118–1125.

Gurunathan, S., Han, J.W., Eppakayala, V., Kim, J.-H., 2013. Microbial reduction of graphene oxide by *Escherichia coli*: a green chemistry approach. Colloids Surf. B: Biointerf. 102, 772–777.

Halawany, H.S., 2012. A review on miswak (*Salvadora persica*) and its effect on various aspects of oral health. Saudi Dent. J. 24, 63–69.

Han, T.H., Khan, M.M., Kalathil, S., Lee, J., Cho, M.H., 2013. Synthesis of positively charged gold nanoparticles using a stainless-steel mesh. J. Nanosci. Nanotechnol. 13, 6140–6144.

Hebbalalu, D., Lalley, J., Nadagouda, M.N., Varma, R.S., 2013. Greener techniques for the synthesis of silver nanoparticles using plant extracts, enzymes, bacteria, biodegradable polymers, and microwaves. ACS Sustain. Chem. Eng. 1, 703–712.

Herves, P., Pérez-Lorenzo, M., Liz-Marzán, L.M., Dzubiella, J., Lu, Y., Ballauff, M., 2012. Catalysis by metallic nanoparticles in aqueous solution: model reactions. Chem. Soc. Rev. 41, 5577–5587.

Hsu, K.-C., Chen, D.-H., 2014. Green synthesis and synergistic catalytic effect of Ag/reduced graphene oxide nanocomposite. Nanoscale Res. Lett. 9, 1–10.

Hulkoti, N.I., Taranath, T., 2014. Biosynthesis of nanoparticles using microbes – a review. Colloids Surf. B: Biointerf. 121, 474–483.

Khan, M., Al-Marri, A.H., Khan, M., Mohri, N., Adil, S.F., Al-Warthan, A., Siddiqui, M.R.H., Alkhathlan, H.Z., Berger, R., Tremel, W., 2014a. Pulicaria glutinosa plant extract: a green and eco-friendly reducing agent for the preparation of highly reduced graphene oxide. RSC Adv. 4, 24119–24125.

Khan, M., Al-Marri, A.H., Khan, M., Shaik, M.R., Mohri, N., Adil, S.F., Kuniyil, M., Alkhathlan, H.Z., Al-Warthan, A., Tremel, W., Tahir, M.N., Siddiqui, M.R.H., 2015a. Green approach for the effective reduction of graphene oxide using *Salvadora persica* L. root (miswak) extract. Nanoscale Res. Lett. 10, 281.

Khan, M., Khan, M., Adil, S.F., Tahir, M.N., Tremel, W., Alkhathlan, H.Z., Al-Warthan, A., Siddiqui, M.R.H., 2013a. Green synthesis of silver nanoparticles mediated by *Pulicaria glutinosa* extract. Int. J. Nanomed. 8, 1507–1516.

Khan, M., Khan, M., Kuniyil, M., Adil, S.F., Al-Warthan, A., Alkhathlan, H.Z., Tremel, W., Tahir, N.M., Siddiqui, M.R.H., 2014b. Biogenic synthesis of palladium nanoparticles using *Pulicaria glutinosa* extract and their catalytic activity towards the Suzuki coupling reaction. Dalton Trans. 43, 9026–9031.

Khan, M.E., Khan, M.M., Cho, M.H., 2015b. Green synthesis, photocatalytic and photoelectrochemical performance of an Au–Graphene nanocomposite. RSC Adv. 2015 (5), 26897–26904.

Khan, M.M., Ansari, S.A., Ansari, M.O., Min, B., Lee, J., Cho, M.H., 2014c. Biogenic fabrication of Au@ CeO_2 nanocomposite with enhanced visible light activity. J. Phy. Chem. C 118, 9477–9484.

Khan, M.M., Kalathil, S., Han, T.H., Lee, J., Cho, M.H., 2013b. Positively charged gold nanoparticles synthesized by electrochemically active biofilm – a biogenic approach. J. Nanosci. Nanotechnol. 13, 6079–6085.

Kuila, T., Bose, S., Mishra, A.K., Khanra, P., Kim, N.H., Lee, J.H., 2012. Chemical functionalization of graphene and its applications. Prog. Mater. Sci. 57, 1061–1105.

Kuila, T., Mishra, A.K., Khanra, P., Kim, N.H., Lee, J.H., 2013. Recent advances in the efficient reduction of graphene oxide and its application as energy storage electrode materials. Nanoscale 5, 52–71.

Leng, J., Wang, W.-M., Lu, L.-M., Bai, L., Qiu, X.-L., 2014. DNA-templated synthesis of PtAu bimetallic nanoparticle/graphene nanocomposites and their application in glucose biosensor. Nanoscale Res. Lett. 9 (99), 1–8.

Li, W., Wang, F., Liu, Y., Wang, J., Yang, J., Zhang, L., Elzatahry, A. A., Al-Dahyan, D., Xia, Y., Zhao, D., 2015. General strategy to synthesize uniform mesoporous TiO_2/graphene/mesoporous TiO_2 sandwich-like nanosheets for highly reversible lithium storage. Nano Lett. 15 (3), 2186–2193.

Luo, B., Zhi, L., 2015. Design and construction of three dimensional graphene-based composites for lithium ion battery applications. Energy Environ. Sci. 8, 456–477.

Mahmood, N., Zhang, C., Yin, H., Hou, Y., 2014. Graphene-based nanocomposites for energy storage and conversion in lithium batteries, super capacitors and fuel cells. J. Mater. Chem. A 2, 15–32.

Makarov, V.V., Makarova, S.S., Love, A.J., Sinitsyna, O.V., Dudnik, A.O., Yaminsky, I.V., Taliansky, M.E., Kalinina, N.O., 2014. Biosynthesis of stable iron oxide nanoparticles in aqueous extracts of *Hordeum vulgare* and *Rumex acetosa* plants. Langmuir 30, 5982–5988.

Nadagouda, M.N., Varma, R.S., 2007. A greener synthesis of core (Fe, Cu)-shell (Au, Pt, Pd, and Ag) nanocrystals using aqueous vitamin C. Cryst. Growth Des. 7, 2582–2587.

Navalon, S., Dhakshinamoorthy, A., Alvaro, M., Garcia, H., 2014. Carbocatalysis by graphene-based materials. Chem. Rev. 114, 6179–6212.

Sedki, M., Mohamed, M.B., Fawzy, M., Abdelrehim, D.A., Abdel-Mottaleb, M.M., 2015. Phytosynthesis of silver–reduced graphene oxide (Ag–RGO) nanocomposite with an enhanced antibacterial effect using *Potamogeton pectinatus* extract. RSC Adv. 5, 17358–17365.

Stankovich, S., Dikin, D.A., Dommett, G.H., Kohlhaas, K.M., Zimney, E.J., Stach, E.A., Piner, R., Nguyen, S.T., Ruoff, R.S., 2006. Graphene-based composite materials. Nature 442, 282–286.

Tang, M., Wang, X., Wu, F., Liu, Y., Zhang, S., Pang, X., Li, X., Qiu, H., 2014. Au nanoparticle/graphene oxide hybrids as stabilizers for Pickering emulsions and Au nanoparticle/graphene oxide@polystyrene microspheres. Carbon 71, 238–248.

Ullah, K., Ye, S., Lei, Z., Cho, K.-Y., Oh, W.-C., 2015. Synergistic effect of $PtSe_2$ and graphene sheets supported by TiO_2 as cocatalysts synthesized via microwave techniques for improved photocatalytic activity. Cat. Sci. Technol. 5, 184–198.

Vashist, S.K., Luong, J.H., 2015. Recent advances in electrochemical biosensing schemes using graphene and graphene-based nanocomposites. Carbon 84, 519–550.

Wang, Y., Polavarapu, L., Liz-Marzán, L.M., 2014. Reduced graphene oxide-supported gold nanostars for improved SERS sensing and drug delivery. ACS Appl. Mater. Interf. 6, 21798–21805.

Xia, B., Yan, Y., Wang, X., Lou, X.W.D., 2014. Recent progress on graphene-based hybrid electrocatalysts. Mater. Horiz. 1, 379–399.

Xu, C., Wang, X., Zhu, J., 2008. Graphene–metal particle nanocomposites. J. Phys. Chem. C 112, 19841–19845.

Yin, P.T., Shah, S., Chhowalla, M., Lee, K.-B., 2015. Design, synthesis, and characterization of graphene–nanoparticle hybrid materials for bioapplications. Chem. Rev. 115, 2483–2531.

Zhang, C., Zhu, X., Wang, Z., Sun, P., Ren, Y., Zhu, J., Zhu, J., Xiao, D., 2014a. Facile synthesis and strongly microstructure-dependent electrochemical properties of graphene/manganese dioxide composites for supercapacitors. Nanoscale Res. Lett. 9 (490), 1–8.

Zhang, H., Hines, D., Akins, D.L., 2014b. Synthesis of a nanocomposite composed of reduced graphene oxide and gold nanoparticles. Dalton Trans. 43, 2670–2675.

Zhu, Y., Murali, S., Cai, W., Li, X., Suk, J.W., Potts, J.R., Ruoff, R. S., 2010. Graphene and graphene oxide: synthesis, properties, and applications. Adv. Mater. 22, 3906–3924.